CrossMark

Improvement in microwave dielectric properties of Sr_2TiO_4 ceramics through post-annealing treatment

Yu Luo[1] · Jie Zhang[1] · Zhenxing Yue[1] · Longtu Li[1]

Abstract

Sr_2TiO_4 ceramics were synthesized via the conventional solid-state reaction process, and the effects of post-annealing treatment in air on the microwave dielectric properties and defect behavior of title compound were investigated systematically. The $Q \times f$ values could be effectively improved from 107,000 GHz to 120,300 GHz for the specimens treated at 1450 °C for 16 h. The thermally stimulated depolarization currents (TSDC) revealed two kinds of defect dipoles [$\left(Ti^{'}_{Ti} - V^{\bullet\bullet}_O \right)$ and $\left(V^{\wedge}_{Sr} - V^{\bullet\bullet}_O \right)$] and oxygen vacancies $\left(V^{\bullet\bullet}_O \right)$ were considered the main defects in Sr_2TiO_4. Under a post-annealing treatment in air, the concentrations of such defects in the ceramics decreased. Meanwhile, the impedance spectrum revealed the activation energy of the grain boundaries increased. These evidences could account for the improvement of $Q \times f$ values. Accompanied with a high ε_r of 40.4 and a large τ_f of 126 ppm/°C, the enhanced high-Q Sr_2TiO_4 ceramics can be good candidates for applications in wireless passive temperature sensing.

Keywords Microwave dielectrics · Post-annealing · Thermally-stimulated relaxations · Defects

1 Introduction

Over the past several decades, microwave dielectrics with temperature coefficient of resonant frequency (τ_f) around zero have been widely used in commercial microwave devices, such as dielectric resonators and filters [1]. Recently, microwave dielectrics with high-τ_f have received much attention for applications in wireless passive temperature sensors because of their high sensitivity to temperature [2, 3]. This wireless passive temperature sensor based on microwave dielectrics could detect the changes in resonant frequency with temperature by sending a wideband signal and receiving a reflection from the sensors, so that it allows to determine the environmental temperature changes [4, 5]. The temperature sensing mechanism offers great potential for such sensors to operate in harsh environment such as high-speed spinning mechanical components.

Generally, microwave dielectrics with high dielectric constant (ε_r), high Q and high τ_f are preferred for the wireless passive temperature sensors. Recently, Al_2O_3 ceramics were reported to perform well for temperature sensing [2]. However, it has a relatively low ε_r ~10 and a low τ_f value ~ −60 ppm/°C, which is not suitable for the miniaturization and sensitivity of the wireless passive temperature sensor. As well, $MgTiO_3$ ($\varepsilon_r = 17$, $Q \times f = 160,000$ GHz and $\tau_f = -50$ ppm/°C) [6], Mg_2TiO_4 ($\varepsilon_r = 14$, $Q \times f = 150,000$ GHz and $\tau_f = -50$ ppm/°C) [7] are not suitable for temperature sensing, despite of their high $Q \times f$ values and relatively low sintering temperatures.

Sr_2TiO_4 ceramics possess a high ε_r of ~ 40, a high $Q \times f$ value >100,000 GHz and a high τ_f value >100 ppm/°C, which can be a promising material used for wireless passive temperature sensing. Thus, Sr_2TiO_4 was chosen as the fundamental materials in the present work. Importantly, microwave dielectrics are required to have a high $Q \times f$ value to allow higher resolution and wider sensing distance for the sensors. For the purpose of further improving the $Q \times f$ value for Sr_2TiO_4 ceramics, the underlying loss mechanisms including defects relaxation behavior need consideration. Several works have been reported on the microwave dielectric properties of Sr_2TiO_4 ceramics [8], but very few of them suggest the post-treatment process to improve their microwave dielectric properties. Besides,

✉ Jie Zhang
zjie.mse@gmail.com

✉ Zhenxing Yue
yuezhx@mail.tsinghua.edu.cn

[1] State Key Laboratory of New Ceramics and Fine Processing, School of Materials Science and Engineering, Tsinghua University, Beijing 100084, People's Republic of China

the types of defects in Sr_2TiO_4 and related information remain unclear. Hence, it is important to investigate the defects relaxation behavior in Sr_2TiO_4, and therefore to seek for effective ways to improve the microwave dielectric properties.

More recently, the thermally stimulated depolarization current (TSDC) technique has been considered a useful tool in the study and quantification of defects (trap charge, dipole, and oxygen vacancy) in dielectrics [3, 9–11]. Additionally, impedance spectrum is helpful to monitor the defect-associated mechanisms of the materials. Therefore, the two techniques were combined to study the defects behaviors in Sr_2TiO_4 ceramics with a post-annealing treatment process. Here the extrinsic dielectric loss mechanisms in Sr_2TiO_4 ceramics were investigated, and the counterparts with enhanced high-Q after post-annealing can be good candidates for applications in wireless passive temperature sensing.

2 Experiment procedure

The Sr_2TiO_4 ceramics are prepared via the conventional solid-state reaction processing using high-purity $SrCO_3$ (99.95%) and TiO_2 (99.99%) powders as the starting materials. The stoichiometric $SrCO_3$ and TiO_2 powders were mixed and ground together with ethanol medium for 4 h in a ball mill. After drying and sieving, the mixture was calcined at 1300 °C for 4 h, as the precursor powders. The calcined powders were ball mixed in ethanol for 4 h and dried. The final powders were uniaxially pressed together with an organic binder (5 wt% polyvinyl alcohol) under 200 MPa into cylinders and pellets with appropriate specifications. These samples were sintered at 1550 °C for 4 h in air. The sintered ceramics were heated at 1450 °C for 4–16 h in the post-annealing treatment.

The crystal phases of the ceramics were characterized using X-ray diffraction (XRD) analysis with CuK_α radiation (D8 Advanced; Bruker, Karlsruhe, Germany). The microstructures of the samples were investigated by scanning electron microscopy (SEM, MERLIN VP Compact, Zeiss, Germany). A network analyzer (HP8720ES, Hewlett-Packard, Santa Rosa, CA, USA) was used to measure the microwave dielectric properties of the samples. The dielectric constants were measured using the Hakki-Coleman [12] post resonator method by exciting the TE_{011} resonant mode of the dielectric resonators using the electric probe of an antenna as suggested by Courtney [13]. The unloaded quality factors were measured using the $TE_{01\delta}$ mode in the cavity method [14]. The temperature coefficients of the resonant frequencies of the TE_{011} mode were obtained in the temperature

range of 25 °C–80 °C. The τ_f values were calculated using the following relationship:

$$\tau_f = \frac{f_2 - f_1}{f_1(T_2 - T_1)} \tag{1}$$

where f_1 and f_2 are the resonant frequency at T_1 (25 °C) and T_2 (80 °C), respectively.

For the dielectric and TSDC measurements, the surfaces of the pellets were polished and silver electrodes were applied on both sides. TSDC measurements were performed using a pA meter (6517B, Keithley, Cleveland, Ohio, USA), and temperature-dependent measurements were performed using a quatro temperature controller (Novocontrol, Montabaur, Germany). Complex impedance was measured by a precision LCR meter (Keysight, E4980AL, USA) over frequencies from 20 Hz to 10 MHz in a temperature range of 440– 520 °C. The evaluation of each R (resistance) and C (capacitance) component value for an assumed equivalent circuit was determined by software Z-VIEW (version 2.3).

3 Result and discussion

Fig. 1 shows the XRD patterns of the sintered Sr_2TiO_4 ceramics and post-annealed ceramics. Both patterns exhibit a pure Sr_2TiO_4 phase (JCPDS 72–2040) and no additional peak associated with secondary phase is observed, indicating that there is no phase transition in the post-annealing treatment.

The SEM images of the Sr_2TiO_4 ceramics with post-annealing for 0 h, 4 h, 8 h and 16 h are shown in Fig. 2. For all the samples, they have relatively dense microstructures with low porosity. As the post-annealing time increases, the grains size of the samples increases slightly. These results indicate that ceramics were well-sintered under the
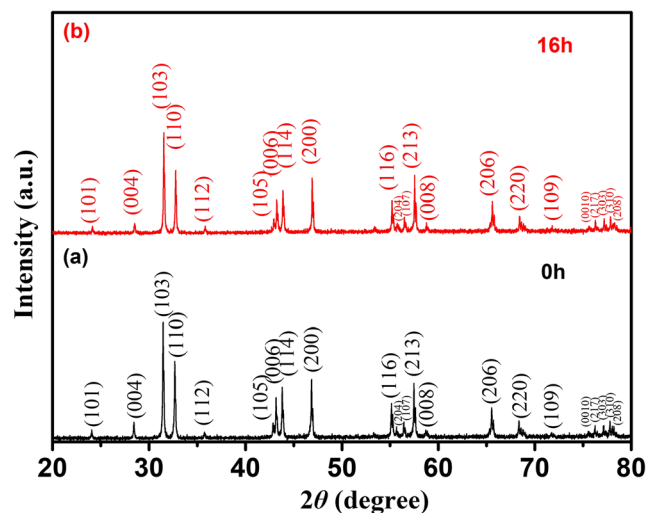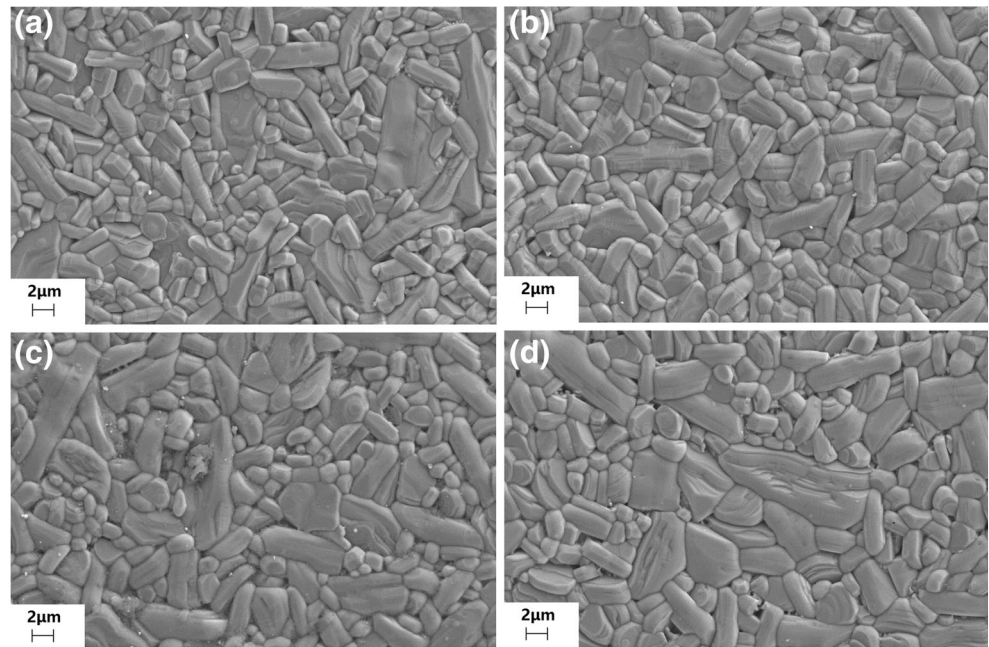

Fig. 1 XRD patterns of Sr_2TiO_4 ceramics with different post-annealing time: (a) 0 h and (b) 16 h

Fig. 2 SEM images of the Sr$_2$TiO$_4$ ceramics with different post-annealing time: (**a**) 0 h, (**b**) 4 h, (**c**) 8 h and (**d**) 16 h

experiment procedure and the grains growth could be slightly enhanced by the post-annealing treatment.

Fig. 3 shows the relative densities and the microwave dielectric properties of the Sr$_2$TiO$_4$ ceramics with post-annealing for different time. Fig. 3a shows that the relative densities decrease slowly with increasing the post-annealing time. As shown in the SEM images (Fig. 2), the grains with strip shapes tend to bridge each other. As the post-annealing time increases, the grain size increases slightly and the pores between the bridging grains become large to some extent. This would increase the porosity in the ceramics and lower the relative densities. All the relative densities of the Sr$_2$TiO$_4$ ceramics are higher than 98%, which agrees with the dense microstructure showed in the SEM images of Fig. 2. Fig. 3b shows ε_r as a function of the post-annealing time for the Sr$_2$TiO$_4$ ceramics. It indicates that ε_r decreases slightly from 40.8 to 40.4 with the post-annealing time increasing from 0 h to 16 h, which behaves a similar trend with the relative density. This similarity reveals that the porosity acts as the dominating factor on ε_r. As shown in Fig. 3c, the $Q \times f$ values increase rapidly from 107,000 GHz to 116,000 GHz with the very first post-annealing for 4 h, and then ascend gradually with further increasing the post-annealing time. After post-annealing for 16 h, the $Q \times f$ values can be effectively improved to 120,300 GHz, which has increased by 12.4% comparing with the counterparts without post-annealing. The variation of τ_f values against the post-annealing time is given in Fig. 4d. As the post-annealing time increases, the τ_f values decrease slowly from +131 ppm/°C to +126 ppm/°C, which is associated with the decrease of the dielectric constant [15]. These results show that the post-annealing treatment has a
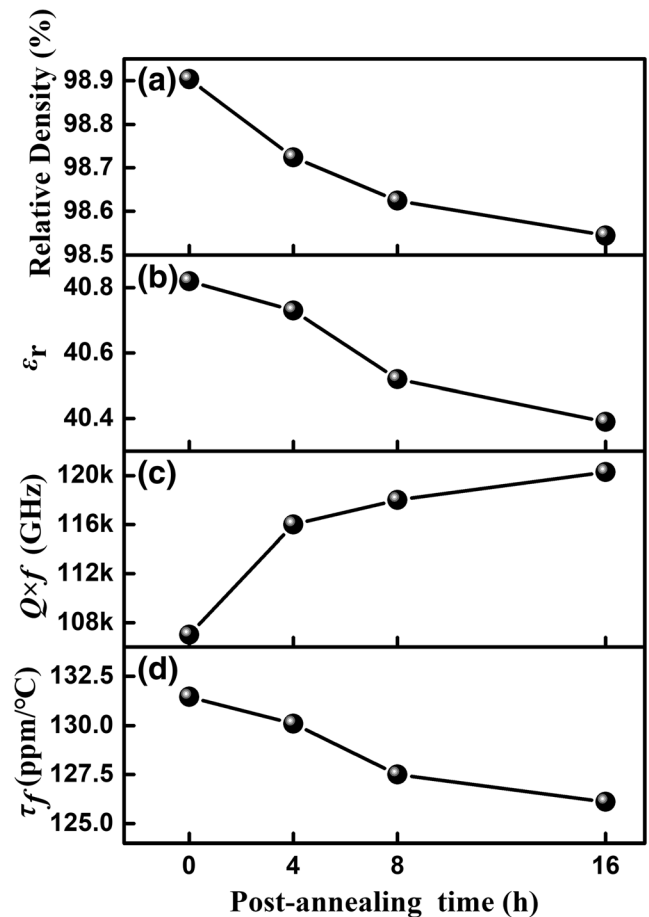

Fig. 3 Relative densities and microwave dielectric properties of Sr$_2$TiO$_4$ ceramics vs post-annealing time: (**a**) relative densities, (**b**) dielectric constant, (**c**) $Q \times f$ values and (**d**) τ_f values
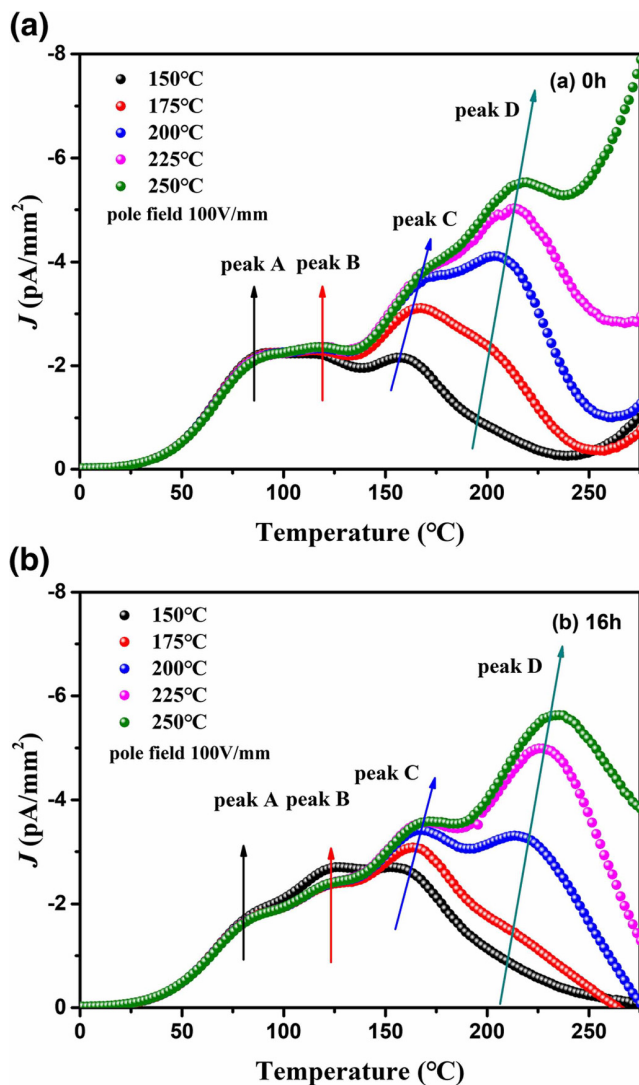
(a)

(b)

Fig. 4 TSDC curves of Sr$_2$TiO$_4$ ceramics with different post-annealing time: (**a**) 0 h and (**b**) 16 h
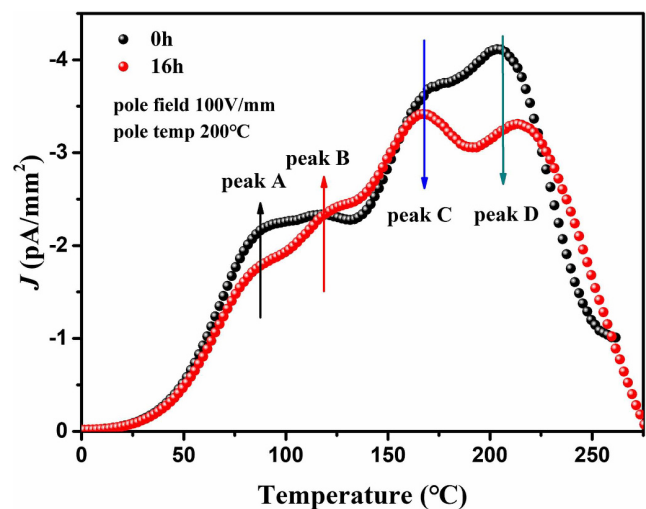

Fig. 5 TSDC curves of the ceramics with post-annealing for 0 h and 16 h under the same polarization conditions ($E_p = 100$ V/mm, $T_p = 200$ °C)

100 V/mm and different polarization temperatures (T_p, from 150 °C to 250 °C). Basically, four distinct relaxation peaks (peaks A, B, C and D) are found in each curve. It suggests that at least four kinds of defect relaxation mechanisms exist in Sr$_2$TiO$_4$. As T_p increases, the T_m (the temperature at which the maximum peak value occurs) of peak A do not change, as shown by the arrow. Peak B shares a similar trend with peak A. This result indicates that peak A and peak B are more related to defect dipoles [9, 10]. In the Ti-containing ceramics, the oxygen loss and the reduction of Ti are generally considered to be the most possible origins of oxygen vacancies during the sintering process [16, 17]. Using standard Kröger–Vink notation, the equation of the reduction of Ti can be described as follow:

$$2\text{Ti}_{\text{Ti}} + \text{O}_{\text{o}} \rightarrow 2\text{Ti}'_{\text{Ti}} + V_{\text{O}}^{\bullet\bullet} + \frac{1}{2}\text{O}_2 \tag{2}$$
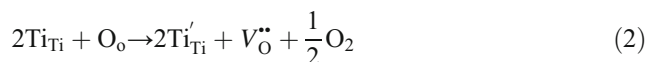
Based on the relevant literatures, the defect dipoles $\left(V_{\text{Ba,Sr}}^{\wedge} - V_{O}^{\bullet\bullet}\right)$ have been found in Ba$_{0.6}$Sr$_{0.4}$TiO$_3$ ceramics [18]. It suggests that the two kinds of defect dipoles in Sr$_2$TiO$_4$ are likely to be $\left(\text{Ti}'_{\text{Ti}} - V_{O}^{\bullet\bullet}\right)$ and $\left(V_{\text{Sr}}^{\wedge} - V_{O}^{\bullet\bullet}\right)$. Because little work has been reported on the defect dipoles of Sr$_2$TiO$_4$, each kind of defect dipoles could not be assigned to a certain peak (peak A or peak B), which need a further research. For peak C and peak D, both T_m and J_m (peak of the current density) increase with increasing T_p, indicating that the two peaks more likely arise from the relaxation of mobile oxygen vacancies [16, 17]. In polycrystalline ceramics, generally, the relaxations of oxygen vacancies can be divided into two types: the in-grain relaxations and across-grain-boundary relaxations [19]. As T_p increases, the oxygen vacancies migrate in grains are gradually blocked by the grain boundaries, leading to a
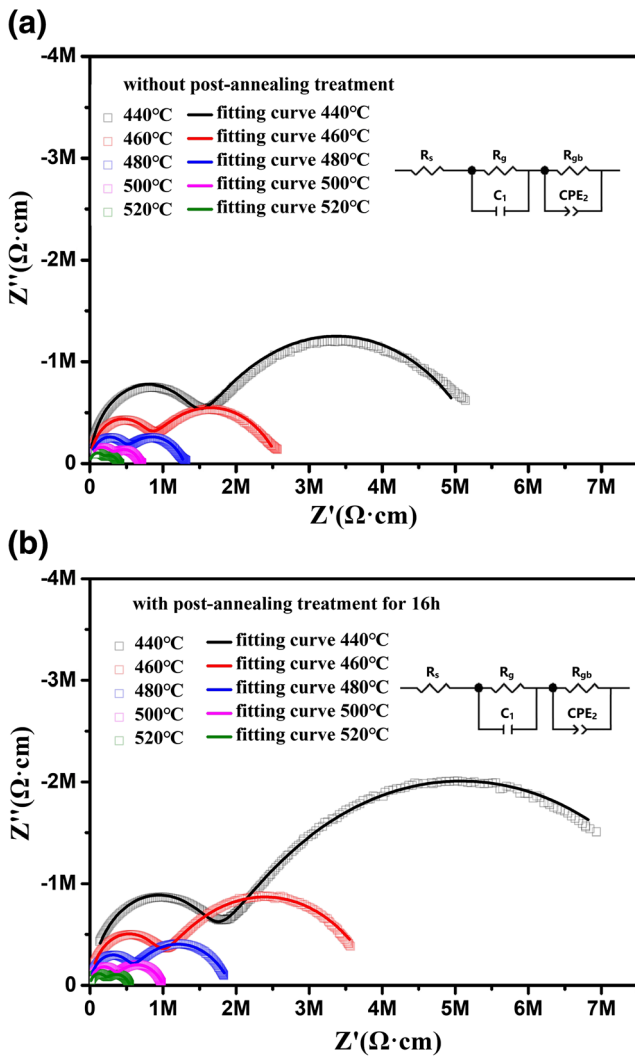
slight effect on ε_r and τ_f values, and could improve the $Q \times f$ values effectively. With a high ε_r of 40.4 and a large τ_f of 126 ppm/°C, the enhanced high-Q Sr$_2$TiO$_4$ ceramics can be good candidates for applications in wireless passive temperature sensing. The variation in $Q \times f$ values with post-annealing treatment should mainly attribute to the extrinsic factors such as porosity, grain size, oxygen vacancy, etc. The ceramics with and without the treatment both have relatively high densification (> 98%), and the grain size changes slightly after the treatment, so the effect of porosity and the grain size on microwave dielectric loss can be neglected. To investigate the possible reason for the apparent enhancement in $Q \times f$ values, TSDC measurements and impedance spectrum were performed on the Sr$_2$TiO$_4$ ceramics with post-annealing for 0 h and 16 h.

Fig. 4a shows the TSDC curves for Sr$_2$TiO$_4$ ceramics without post-annealing under a fixed polarization field (E_p) of

Fig. 6 Impedance spectrums of Sr_2TiO_4 ceramics with different post-annealing time: (**a**) 0 h and (**b**) 16 h

Fig. 7 Arrhenius plots of ln$R$ versus $1/kT$ of Sr_2TiO_4 ceramics with different post-annealing time: (**a**) 0 h and (**b**) 16 h. The activation energy is calculated from the slope. E_{Rg} denotes the activation energy of the grain, E_{Rgb} denotes the activation energy of the grain boundary

saturation of J_m. Further increasing T_p causes oxygen vacancies migrate across the grain boundaries and a further increased J_m [3]. Figure 4a shows that both T_m and J_m increase rapidly with T_p at first and then saturate for peak C. As for peak D, T_m has the similar trend, but its J_m increases without saturating. These results indicate that peak C is associated with the relaxations of in-grain oxygen vacancies and peak D is associated with the relaxations of across-grain-boundary oxygen vacancies [9–11]. Therefore, the two kinds of defect dipoles [$\left(Ti'_{Ti}-V_O^{\bullet\bullet}\right)$ and $\left(V_{Sr}^{\wedge}-V_O^{\bullet\bullet}\right)$] and oxygen vacancies $\left(V_O^{\bullet\bullet}\right)$ are considered the main defects in Sr_2TiO_4. Figure 4b shows the TSDC curves for Sr_2TiO_4 ceramics with post-annealing for 16 h. The corresponding four distinct relaxation peaks (peaks A, B, C and D) are found in each curve. The analysis described above suggests that the Sr_2TiO_4 ceramics with post-annealing for 16 h have the similar kinds of defects with the Sr_2TiO_4 ceramics without post-annealing.
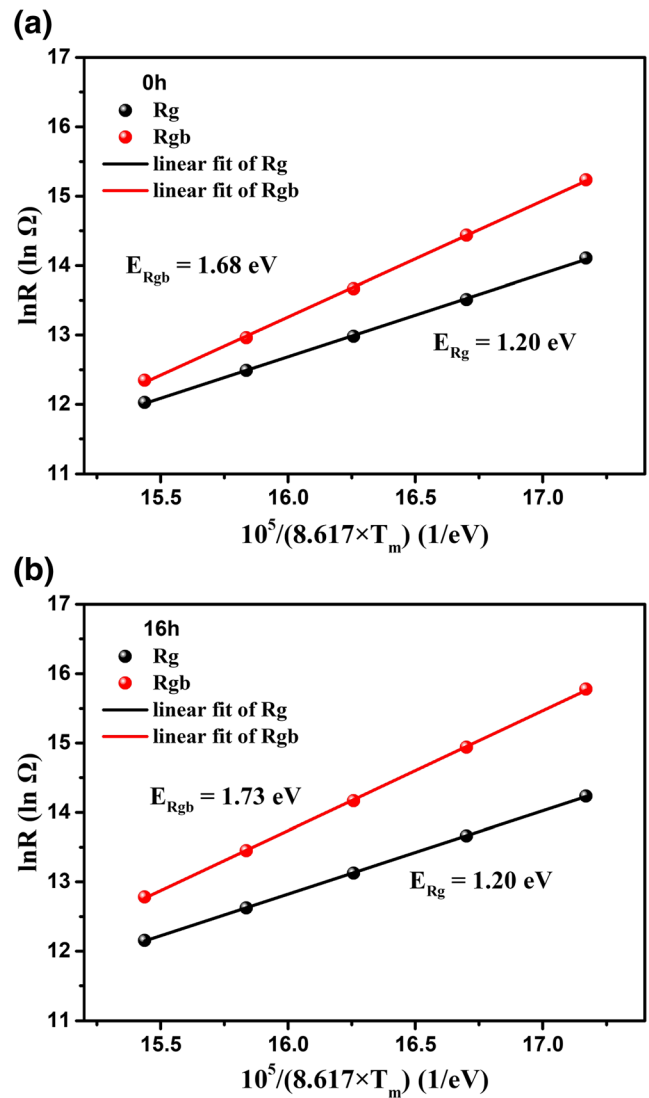
To investigate the effect of the post-annealing treatment on the defect behavior of Sr_2TiO_4 ceramics, the TSDC curves of the samples with different post-annealing times are compared. Figure 5 shows the TSDC curves of the Sr_2TiO_4 ceramics with post-annealing for 0 h and 16 h under the same polarization conditions ($E_p = 100$ V/mm, $T_p = 200$ °C). With the post-annealing time increasing from 0 h to 16 h, the J_m of peaks A, C and D increase obviously. According to the Langevin function [20], TSDC peaks with higher intensity indicate higher defect concentrations. Therefore, under a post-annealing treatment in air, the concentrations of the defects in the Sr_2TiO_4 ceramics decrease. Since the defects, particularly oxygen vacancies, are considered to generate inharmonic vibrations and cause extrinsic dielectric loss consequently [21–23]. The results of the TSDC curves are consistent with the microwave dielectric characters.

The impedance analysis was performed on the selected samples under a series of temperatures from 440 °C to 520 °C and a frequency range of 20 Hz to 10 MHz. Figure 6 shows the impedance spectra of the Sr_2TiO_4 ceramics with post-annealing for 0 h and 16 h. Referring to the previous study [24–26], an equivalent circuit of 2RC elements is selected to describe the impedance spectra, as shown in the inset of Fig. 6. This equivalent circuit is assigned to grains and grain boundaries, which the contribution positioned at low frequencies corresponds to the grain boundaries response and that at high frequencies corresponds to the grains response. In order to obtain reasonable fitting results, the constant phase element (CPE) is considered in the equivalent circuit. The resistance of the grain and grain boundaries at various temperatures could be evaluated by fitting the experimental data. As illustrated in Fig. 6, the measured data are well-matched to the calculated data, indicating that the equivalent circuit is reasonable to analyze the impedance spectra. Based on the pertinent literature [27], the activation energies of grains and grain boundaries can be determined from Arrhenius equation, as presented in Eq. (3).

$$R = R_0 \exp\left(\frac{E_a}{kT}\right) \qquad (3)$$

Here, R_0 is a constant, E_a is the activation energy, k is the Boltzmann constant, and T is the absolute temperature.

Fig. 7 shows the activation energies of grains and grain boundaries for the Sr_2TiO_4 ceramic. When the post-annealing time increases from 0 h to 16 h, the activation energy of grains does not change while the activation energy of grain boundaries increases from 1.68 eV to 1.73 eV. The result could be derived from the chemical defects concentrations at grain boundaries decrease with post-annealing treatment and therefore grain boundaries become less electrically active. It is good for the improvement in the $Q \times f$ values of the ceramics and agrees with the microwave dielectric properties.

4 Conclusion

Significant TSDC relaxations (peaks A, B, C, and D) were observed in Sr_2TiO_4 ceramics which were synthesized by the solid-state reaction method. The main defects in Sr_2TiO_4 ceramics appeared to be two kinds of defect dipoles [$\left(Ti'_{Ti}-V_O^{\bullet\bullet}\right)$ and $\left(V_{Sr}^{\wedge}-V_O^{\bullet\bullet}\right)$] and oxygen vacancies $\left(V_O^{\bullet\bullet}\right)$. Under a post-annealing treatment in air, the concentrations of such defects in Sr_2TiO_4 decreased. Additionally, the impedance spectrum revealed the activation energy of the grain boundaries increased after post-annealing. The $Q \times f$ values could be effectively improved from 107,000 GHz to 120,300 GHz for the specimens treated at 1450 °C for 16 h. With the enhanced $Q \times f$ values, the materials also have a high ε_r of 40.4 and a high τ_f value of +126 ppm/°C, possessing good potential for applications in wireless passive temperature sensing.

References

1. M.T. Sebastian, *Dielectric Materials for Wireless Communication* (Elsevier, UK, 2010)
2. H.T. Cheng, S. Ebadi, X. Gong, IEEE Antennas Wireless Propag. Lett. **11**, 369–372 (2012)
3. J. Zhang, Z.X. Yue, Y.Y. Zhou, B. Peng, X.H. Zhang, L.T. Li, J. Eur. Ceram. Soc. **36**(8), 1923–1930 (2016)
4. H. Cheng, S. Ebadi, X. Ren, Y. Yusuf, X. Gong, IEEE AP-S Int. Symp. 1350 (2011)
5. Y. Wang, Y. Jia, Q. Chen, Y. Wang, Sensors **8**(12), 7982–7995 (2008)
6. K. Wakino, Ferroelectrics **91**(1), 69–86 (1989)
7. A. Belous, O. Ovchar, J. Am. Ceram. Soc. **89**(11), 3441–3445 (2006)
8. B. Liu, L. Li, X.Q. Liu, X.M. Chen, J. Am. Ceram. Soc. **100**(2), 496–500 (2017)
9. W. Liu, C.A. Randall, J. Am. Ceram. Soc. **91**(10), 3245–3250 (2008)
10. W. Liu, C.A. Randall, J. Am. Ceram. Soc. **91**(10), 3251–3257 (2008)
11. J. Zhang, Z.X. Yue, Y.Y. Zhou, X.H. Zhang, L.Y. Li, J. Am. Ceram. Soc. **98**(12), 3942–3947 (2015)
12. B.W. Hakki, P.D. Coleman, IRE Trans. Microwave Theory Tech. **8**(4), 402–410 (1960)
13. W.E. Courtney, IEEE Trans. Microwave Theory Tech. **18**(8), 476–485 (1970)
14. J. Krupka, K. Derzakowski, B. Riddle, J. Baker-Jarvis, Meas. Sci. Technol. **9**(10), 1751–1756 (1998)
15. A.J. Moulson, J.M. Herbert, *Electroceramics: Materials, Properties and Applications* (Wiley, New York, 2003)
16. A. Templeton, X. Wang, S.J. Penn, S.J. Webb, L.F. Cohen, N.M.N. Alford, J. Am. Ceram. Soc. **83**(1), 95–100 (2000)
17. R.C. Pullar, S.J. Penn, X. Wang, I.M. Reaney, N.M.N. Alford, J. Eur. Ceram. Soc. **29**(3), 419–424 (2009)
18. T. Teranishi, R. Kanemoto, H. Hayashi, A. Kishimoto, J. Am. Ceram. Soc. **100**(3), 1037–1043 (2017)
19. S.H. Yoon, C.A. Randall, K.H. Hur, J. Am. Ceram. Soc. **93**, 1950 (2010)
20. P. Bräunlich, *Topics in Applied Physics: Thermally Stimulated Relaxation in Solids*. 37, (1979)
21. I.M. Reaney, D. Iddles, J. Am. Ceram. Soc. **89**, 2063 (2006)
22. H. Tamura, J. Eur. Ceram. Soc. **26**(10-11), 1775–1780 (2006)
23. J.D. Breeze, J.M. Perkins, D.W. McComb, N.M. Alford, J. Am. Ceram. Soc. **92**(3), 671–674 (2009)
24. A.R. West, D.C. Sinclair, N. Hirose, J. Electroceram. **1**(1), 65–71 (1997)
25. G.Y. Yang, E.C. Dickey, C.A. Randall, D.E. Barber, P. Pinceloup, M.A. Henderson, R.A. Hill, J.J. Beeson, D.J. Skamser, J. Appl. Phys. **96**(12), 7492–7499 (2004)
26. S.H. Yoon, C.A. Randall, K.H. Hur, J. Am. Ceram. Soc. **92**(8), 1758–1765 (2009)
27. H.L. Gong, X.H. Wang, S.P. Zhang, Z.B. Tian, L.T. Li, J. Appl. Phys. **112**(11), 114119 (2012)